JHU/APL
TG 1368
JULY 1988



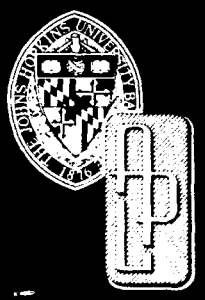

*Technical Memorandum*

# SURVEY OF IMAGE RESTORATION TECHNIQUES

P. K. MURPHY



THE JOHNS HOPKINS UNIVERSITY ■ APPLIED PHYSICS LABORATORY

UNCLASSIFIED

SECURITY CLASSIFICATION OF THIS PAGE

ADA197470

# REPORT DOCUMENTATION PAGE

| | |
|---|---|
| 1a REPORT SECURITY CLASSIFICATION<br>UNCLASSIFIED | 1b RESTRICTIVE MARKINGS |
| 2a SECURITY CLASSIFICATION AUTHORITY | 3 DISTRIBUTION/AVAILABILITY OF REPORT<br>Approved for public release; distribution unlimited |
| 2b DECLASSIFICATION/DOWNGRADING SCHEDULE | |
| 4 PERFORMING ORGANIZATION NUMBER(S)<br>JHU APL TG 1368 | 5 MONITORING ORGANIZATION REPORT NUMBER(S)<br>JHU/APL TG 1368 |
| 6a NAME OF PERFORMING ORGANIZATION<br>The Johns Hopkins University Applied Physics Laboratory<br>6b OFFICE SYMBOL (If Applicable)<br>TIR | 7a NAME OF MONITORING ORGANIZATION<br>NAVPRO, Laurel, Maryland |
| 6c ADDRESS (City, State, and ZIP Code)<br>Johns Hopkins Road<br>Laurel, Maryland 20707 | 7b ADDRESS (City, State, and ZIP Code)<br>Johns Hopkins Road<br>Laurel, Maryland 20707 |
| 8a NAME OF FUNDING/SPONSORING ORGANIZATION<br>NAVAIR<br>8b OFFICE SYMBOL (If Applicable) | 9 PROCUREMENT INSTRUMENT IDENTIFICATION NUMBER<br>N00039-87-C-5301 |
| 8c ADDRESS (City, State, and ZIP Code)<br>Jefferson Plaza<br>Washington, DC 20361 | 10 SOURCE OF FUNDING NUMBERS<br>PROGRAM ELEMENT NO: / PROJECT NO: / TASK NO: M2Q0 / WORK UNIT ACCESSION NO: |

11 TITLE (Include Security Classification)

Survey of Image Restoration Techniques

12 PERSONAL AUTHOR(S)

P. K. Murphy

| 13a TYPE OF REPORT | 13b TIME COVERED | 14 DATE OF REPORT (Year, Month, Day) | 15 PAGE COUNT |
|---|---|---|---|
| Technical Memorandum | FROM 4 86 TO 8 86 | 1988, ~~January~~ July | 35 |

16 SUPPLEMENTARY NOTATION

| 17 COSATI CODES | | | 18 SUBJECT TERMS |
|---|---|---|---|
| FIELD | GROUP | SUB-GROUP | image restoration; Wiener filtering; MAP restoration; deconvolution techniques; inverse filtering; image deblurring; homomorphic deconvolution |

19 ABSTRACT (Continue on reverse if necessary and identify by block number)

This survey of image restoration techniques presents a concise overview of the most useful restoration methods. Linear spatially invariant and linear spatially variant image restoration techniques are described and the strengths and weaknesses of each approach are identified. Examples of restored images for the various techniques are given. To provide guidelines for choosing a restoration technique for a particular application, a comparison of the techniques is made. The restoration methods are compared and evaluated based on the following criteria: restored image visual quality, performance in the presence of additive image-independent noise, degree of a priori knowledge required, and computational complexity.

| 20 DISTRIBUTION/AVAILABILITY OF ABSTRACT | 21 ABSTRACT SECURITY CLASSIFICATION |
|---|---|
| ☒ UNCLASSIFIED/UNLIMITED ☐ SAME AS RPT ☐ DTIC USERS | UNCLASSIFIED |
| 22a NAME OF RESPONSIBLE INDIVIDUAL<br>NAVPRO Security Officer | 22b TELEPHONE (Include Area Code)<br>(301) 953-5403 |
| | 22c OFFICE SYMBOL<br>NAVPRO SE |

DD FORM 1473, 83 APR

83 APR edition may be used until exhausted. All other editions are obsolete.

SECURITY CLASSIFICATION OF THIS PAGE

UNCLASSIFIED

JHU/APL
TG 1368
JULY 1988

*Technical Memorandum*

# SURVEY OF IMAGE RESTORATION TECHNIQUES

P. K. MURPHY

THE JOHNS HOPKINS UNIVERSITY ■ APPLIED PHYSICS LABORATORY
Johns Hopkins Road, Laurel, Maryland 20707
Operating under Contract N00039-87-C-5301 with the Department of the Navy

THE JOHNS HOPKINS UNIVERSITY
APPLIED PHYSICS LABORATORY
LAUREL, MARYLAND

## ABSTRACT

This survey of image restoration techniques presents a concise overview of the most useful restoration methods. Linear spatially invariant and linear spatially variant image restoration techniques are described and the strengths and weaknesses of each approach are identified. Examples of restored images for the various techniques are given. To provide guidelines for choosing a restoration technique for a particular application, a comparison of the techniques is made. The restoration methods are compared and evaluated based on the following criteria: restored image visual quality, performance in the presence of additive image-independent noise, degree of a priori knowledge required, and computational complexity.

# EXECUTIVE SUMMARY

This technical report gives a broad overview of the field of image restoration and focuses on the most commonly used and successful restoration techniques. Comparisons of these techniques are made so that the reader who is faced with a specific application can quickly perform the necessary trade-offs to choose an appropriate restoration method.

Image restoration is defined as the processing performed on a degraded image to remove or reduce the degrading effects. Restoration differs from image enhancement in that it requires prior knowledge of the degradation phenomena. The degradations in an imaging system arise from the filtering effects of the optical elements, electrical components, and surrounding environment.

To lay the foundation for the analytic methods discussed, basic models of imaging systems are introduced in Section 2.0 and the effects of these systems on the original object are identified. Linear spatially variant and invariant as well as spatially separable systems are defined. Since restoration techniques require knowledge of the degrading phenomena, methods for determining these degradations a posteriori from an output blurred image are given in Section 3.0. Methods of direct measurement of the system point spread function from the images of point, line, and edge sources are outlined. Estimation techniques that use homomorphic signal processing concepts are also presented.

The main body of the report, Section 4.0, examines the derivation of linear spatially invariant and variant restoration techniques. The restoration criterion motivating each technique is supplied and the assumptions and limitations of each method are identified. Techniques derived include simple inverse filtering, constrained deconvolution, homomorphic deconvolution, and maximum a posteriori estimation. Superresolution methods are also briefly discussed.

Section 5.0 compares the image restoration techniques considered. The methods are compared against the following criteria: visual restoration quality, noise performance, a priori knowledge, and computational complexity. The information in this section offers guidelines for choosing a restoration technique for a particular application. Conclusions and potential areas for future investigation are discussed in Section 6.0.

# CONTENTS

## FIGURES



## TABLES

# 1.0 INTRODUCTION

This technical memorandum surveys the field of image restoration and lays the theoretical groundwork needed to understand the concepts and alternatives in this branch of image processing. Although the scope of the report is general in nature, the reader with a specific application should be able to quickly compare and contrast the restoration techniques applicable to his or her problem.

## 1.1 DEFINITION OF RESTORATION

Image restoration is defined as the processing performed on the image using *a priori* knowledge of the degrading phenomena to reduce or remove the degrading effects. Restoration differs from image enhancement, which uses primarily ad hoc techniques (frequently nonlinear) to bring out or alter certain aspects of the image. Enhancement techniques include histogram reshaping for gray-level modification, "crispening" to sharpen edges, and thresholding to segment the image. Image restoration, on the other hand, seeks to undo, partially or wholly, the degradation an image has undergone for the purpose of restoring it to its original ideal form.

To undo the degradation, we must have prior knowledge of the degrading process. The *a priori* information required by a restoration technique may simply be a general analytic model for the degrading imaging system. Another method may require detailed information about the system filtering effects and the imaged object and noise characteristics. The degree of prior knowledge available for a specific application will thus influence the choice of restoration technique. In Section 4.0 we consider restoration techniques that vary widely in the degree of prior knowledge required.

Major sources of image degradation and specific restoration examples are identified in this introductory section. The general analytic imaging system models used to derive the restoration approaches are presented in Section 2.0. Section 3.0 discusses the a posteriori determination of the imaging degradations by direct measurement and estimation methods. This information is subsequently used as the prior knowledge requisite for the restoration techniques. Both linear spatially invariant and variant techniques are outlined in Section 4.0, along with a few nonlinear restoration methods. Section 5.0 offers a comparison of the techniques (Table 3 is especially useful) and criteria to consider when choosing a restoration method for a particular application. Conclusions and additional comments are given in Section 6.0.

## 1.2 SOURCES OF IMAGE DEGRADATION

In a real imaging system, the image is degraded by the net effect of numerous degradation phenomena. Individual degradations (other than system noise) are typically modeled as having a linear filtering effect on the original object. In general, the individual degradation effects may interact in a complicated fashion to produce the net effect on the image. However, the overall system degradation is usually modeled as the linearly cascaded effects of the individual degradations present in the system to ensure analytic tractability.

Image degradations arise from a variety of sources, such as imaging system optics and electronics, and surrounding environmental effects. Several major sources of image degradation are:

1. Image motion. When the object or imaging system experiences relative motion during the imaging time of exposure, degradation results. Examples of degradation-inducing motions are random and deterministic camera vibrations, camera rotation, and linear camera motion along a flight path.
2. Turbulent media. Differences in air temperature at varying altitudes cause variations in the air's index of refraction and give rise to the random phenomenon turbulence. Hufnagel and Stanley[1] have characterized the effect of this type of degradation for both long- and short-term exposures.
3. Diffraction-limited optics. The optical elements in the imaging system have a filtering effect on the resulting image.[2] Under very low noise conditions, even the filtering effect caused by an ideal imaging system may be reduced by restoration and resolution beyond the diffraction limit obtained.[3-5]
4. Optical aberrations. Aberrations present in the imaging system also degrade the output image. Resto-

[1] R. E. Hufnagel and N. R. Stanley, "Modulation Transfer Function Associated with Image Transmission through Turbulent Media," *J. Opt. Soc. Am.* **54**, 52-61 (1964).
[2] J. W. Goodman, *Introduction to Fourier Optics*, McGraw-Hill, San Francisco (1968).
[3] T. S. Huang, W. F. Schreiber, and O. J. Tretiak, "Image Processing," *Proc. IEEE* **59**, 1586-1609 (1971).
[4] B. R. Frieden, "Restoring with Maximum Likelihood and Maximum Entropy," *J. Opt. Soc. Am.* **62**, 511-518 (1972).
[5] B. R. Frieden and J. J. Burke, "Restoring with Maximum Entropy II: Superresolution of Photographs of Diffraction-Blurred Impulses," *J. Opt. Soc. Am.* **62**, 1202-1210 (1972).

ration techniques have been developed that reduce the effects of defocus, coma, curvature-of-field, astigmatism, and distortion aberrations.[6-8]

5. Thermal effects. Temperature differentials across the imaging system elements and overall operating temperature changes can cause image degradation. Spherical aberration and a shift in focus have been shown to arise from thermal effects caused by aerodynamic heating in infrared missile seeker systems.[9]

These are only a few of the more important degrading effects. Additional sources of degradation include chromatic aberration, detector nonuniformities, camera shutter effects, and scan jitter in video systems.

### 1.3 APPLICATIONS OF RESTORATION

Image restoration can be applied to many interesting image problems in a wide variety of fields. Most applications today are restricted to data that have been stored on magnetic tape or some other storage medium and processed long after the image was formed. However, the development of rapid algorithms and advanced hardware implementations should make real-time image restoration feasible.

One of the first applications of image restoration was in the 1960s at the California Institute of Technology Jet Propulsion Laboratory. Images returned from the Mariner spacecraft contained geometric distortion created by the vidicon on-board camera.[10] Digital restoration techniques were used to remove the distortion. The algorithm worked by locating registration reseau marks and calculating a coordinate transformation that was subsequently applied to the image.

Since then, restoration techniques have been applied in the diverse areas of medicine (X rays, acoustic imagery), surveillance data (satellite and aircraft imagery), oil exploration (seismic signals), and forensic science (smudged fingerprints). Restoration has even found application in the music world as Stockham demonstrated by restoring Enrico Caruso recordings using homomorphic deconvolution.[11]

## 2.0 IMAGING SYSTEM MODELS

To evaluate and reduce the effects of the image degradations discussed in Section 1.0, a mathematical model for the imaging system is needed. Once a system model has been specified, analytic methods can be used to derive restoration techniques. In this section, we first define the imaging system in general terms and then impose various restrictions on the general system description that lead to analytically tractable models.

---

[6] G. M. Robbins and T. S. Huang, "Inverse Filtering for Linear Shift-Variant Imaging Systems," *Proc. IEEE* **60**, 862–872 (1972).

[7] V. V. Sawchuk, "Space Variant Image Restoration by Coordinate Transformations," *J. Opt. Soc. Am.* **64**, 138–144 (1974).

[8] V. V. Sawchuk and M. J. Peyrovian, "Restoration of Astigmatism and Curvature of Field," *J. Opt. Soc. Am.* **65**, 712–715 (1975).

[9] T. J. Harris, "Evaluation of Environmental Optical Effects on High Speed Hemispherical Domes Using a Ray Trace Model," IRIS APPL TR 0286-1-066 (Apr 1986).

[10] D. A. O'Handley and W. B. Green, "Recent Developments in Digital Image Processing at the Image Processing Laboratory at the Jet Propulsion Laboratory," *Proc. IEEE* **60**, 821–828 (1972).

[11] T. G. Stockham, T. M. Cannon, and R. B. Ingebretsen, "Blind Deconvolution through Digital Signal Processing," Proc. IEEE **63**, 678–692 (1975).

## 2.1 CANONIC IMAGING SYSTEM MODEL

A canonic model of image formation and detection is shown in Fig. 1.[12] The detected image plus noise is

$$g(x_i,y_i) = S_1\{b(x_i,y_i)\} + n_1(x_i,y_i) + S_2\{b(x_i,y_i)\}\, n_2(x_i,y_i) , \quad (1)$$

where $n_1$ and $n_2$ represent signal-independent noise, $n_3 \equiv S_2\{b\}n_2$ is signal-dependent noise, $S_1\{\cdot\}$ is the detector response function, $S_2\{\cdot\}$ is the signal-dependent noise function, and $(x_i,y_i)$ denote coordinates in the image plane. For this canonic model, the functions $S_1$ and $S_2$ may be nonlinear.

The image radiant energy, $b(x_i,y_i)$, is found by operating on the object radiant energy by the system point spread function (psf), $h$, which will be, in general, a nonlinear function of spatial, temporal, and frequency coordinates, as well as the object function, $f$, i.e.,

$$b(x_i,y_i,t_i,\lambda_i) = \int_{-\infty}^{\infty}\int\int\int h(x_i,y_i,t_i,\lambda_i,x_o,y_o,t_o,\lambda_o, f(x_o,y_o,t_o,\lambda_o)) \times dx_o\, dy_o\, dt_o\, d\lambda_o , \quad (2)$$

where $(x_o,y_o)$ are the coordinates in the object plane. Although imaging systems are nonlinear (e.g., typical X-ray photographs), many are approximately linear when within some operating constraints. To obtain a more analytically tractable model, we make the simplifying assumption of linearity and neglect the chromatic effects.

If we restrict the temporal effects to relative motion between the imaging camera and the object during the time of exposure, $T$, they can be incorporated into the spatial coordinate dependency. For example, for object motion described by the functions

$$x_i = m_1(x_o,y_o,t_o) , \quad (3)$$

$$y_i = m_2(x_o,y_o,t_o) ,$$

inverse functions can be found such that

$$t_o = k_1(x_o,y_o,x_i) = k_2(x_o,y_o,y_i) , \quad (4)$$

and the image radiant energy is described only in terms of the object and image spatial coordinates.

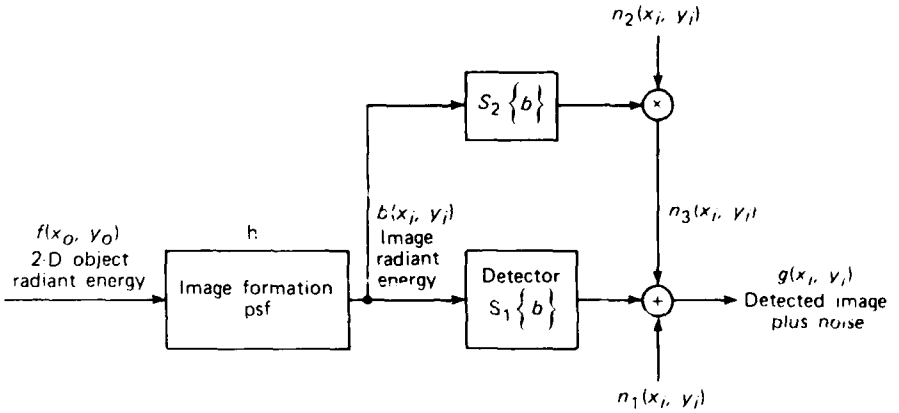


**Figure 1** Canonic imaging system model.

[12] H. C. Andrews and B. R. Hunt, *Digital Image Restoration*, Prentice-Hall, Englewood Cliffs, N.J. (1977).

## 2.2 LINEAR SPATIALLY VARIANT/INVARIANT MODELS

The simplifications discussed in Section 2.1 result in the expression for a linear spatially variant (LSV) imaging system,

$$h(x_i,y_i) = \int_{-\infty}^{\infty}\int h(x_i,y_i,x_o,y_o) \times f(x_o,y_o)\, dx_o\, dy_o \ , \qquad (5)$$

where $h$ is a function of all four spatial variables and has been modified to incorporate any relative motion between object and camera. A common example of an LSV imaging system is one where the camera moves with constant linear velocity normal to the optical axis when imaging a three-dimensional scene. Objects in the foreground will be blurred more than objects in the distance, resulting in spatially variant degradation.

Further simplification results if the system obeys the property of superposition. Then the system is linear spatially invariant (LSI) and

$$h(x_i,y_i) = \int_{-\infty}^{\infty}\int h(x_i - x_o,\, y_i - y_o) \times f(x_o,y_o)\, dx_o\, dy_o \ , \qquad (6)$$

which is the familiar two-dimensional convolution integral. This representation is particularly attractive since it lends itself to Fourier analysis. Consequently, many restoration techniques have been developed for LSI imaging systems.

## 2.3 SPATIALLY SEPARABLE MODELS

Under certain circumstances, the imaging system psf may be spatially separable and

$$h(x_i,y_i,x_o,y_o) = h_1(x_i,x_o)\, h_2(y_i,y_o) \quad (LSV)$$
$$= h_1(x_i - x_o)\, h_2(y_i - y_o) \quad (LSI). \qquad (7)$$

A separable LSI psf might arise, for example, from a unit-square-aperture ideal imaging system,

$$h(x_i,y_i,x_o,y_o) = \left[\frac{\sin\pi(x_i - x_o)}{\pi(x_i - x_o)}\right] \times \left[\frac{\sin\pi(y_i - y_o)}{\pi((y_i - y_o)}\right] . \qquad (8)$$

Separability offers the advantage of performing two-dimensional restoration by sequential one-dimensional operations. This results in a tremendous simplification in the computer implementation of the restoration algorithm.

Other restrictions may be put on the imaging system such as nonnegativity to ensure positive images or lossless imaging constraints. To coincide with digitized computer array representations, we also need to develop a *discrete system model*. A *concise discrete representation* lexicographically orders the $N$ by $N$ two-dimensional object, noise, and image data into one-dimensional vectors each of length $N^2$. The system psf can then be modeled as an $N^2$ by $N^2$ matrix of values $[H]$ resulting in

$$\mathbf{b} = [H]\,\mathbf{f}. \qquad (9)$$

The matrix $[H]$ can be shown to be block Toeplitz for LSI imaging systems.[12] A matrix is Toeplitz if the entries on each diagonal have the same value (i.e., $h_{ij} = h_{kl}$ for $i - j = k - l$); a matrix is block Toeplitz if it has a Toeplitz partitioning and each partition submatrix is also Toeplitz. A summary of the resulting imaging models (noise-free case) for both continuous and discrete systems is given in Table 1.

**Table 1**
Summary of imaging system models.

| | Continuous system | Discrete system |
|---|---|---|
| Noise-free imaging model | $g(x_i,y_i) = \iint h(x_i,y_i,x_o,y_o) f(x_o,y_o) dx_o dy_o$ | $g_{ij} = \sum_k \sum_l h_{ij,kl} f_{kl}$ or $\mathbf{g} = [H]\mathbf{f}$ (lexicographically ordered) |
| Lossless incoherent imaging | $g(x_i,y_i) \geq 0$ | $g_{ij} \geq 0$ |
| | $f(x_o,y_o) \geq 0$ | $f_{kl} \geq 0$ |
| | $h(x_i,y_i,x_o,y_o) \geq 0$ | $h_{ij,kl} \geq 0$ |
| | $\iint h(x_i,y_i,x_o,y_o)\, dx_i\, dy_i = 1$ | $\sum_i \sum_j h_{ij,kl} = 1$ |
| Linear spatially variant | Nonseparable | |
| | $h(x_i,y_i,x_o,y_o) = h(x_i,y_i,x_o,y_o)$ | $[H] = [H]$ |
| | Separable | |
| | $h(x_i,y_i,x_o,y_o) = h_1(x_i,x_o) h_2(y_1,y_o)$ | $[H] = [H_1] \otimes [H_2]$ |
| Linear spatially invariant | Nonseparable | |
| | $h(x_i,y_i,x_o,y_o) = h(x_i - x_o, y_i - y_o)$ | $[H]$ = block Toeplitz |
| | Separable | |
| | $h(x_i,y_i,x_o,y_o) = h_1(x_i - x_o) h_2(y_i - y_o)$ | $[H] = [H_1] \otimes [H_2]$, $[H_1]$, $[H_2]$ Toeplitz |

## 3.0 A POSTERIORI DEGRADATION DETERMINATION

Restoration as defined in Section 1.0 requires a priori knowledge of the degradation performed on the original object. Most of the restoration techniques described in Section 4.0 require knowledge of the imaging system psf. In practical restoration applications, we are commonly faced with the task of a posteriori determination of the degrading psf from the output blurred image.

Various approaches for accomplishing restoration are possible. The techniques outlined below are restricted to LSI imaging system applications. However, if the system is LSV, these techniques can be extended by dividing the image into isoplanatic patches to determine the local psf in each region (see Section 4.3.1 for further discussion). If the original image has a specific struc-

ture, direct measurement of the psf can be performed. Point, line, and edge sources imaged by the system can be used to directly measure or calculate the system psf.[13] Alternately, psf estimation can be accomplished by homomorphic signal processing techniques performed on the blurred image. If a specific parametric form for the degradation is assumed (e.g., linear constant velocity blur, simple optical defocus), estimation techniques that determine the model parameters can be used to develop an expression for the system psf.[12]

## 3.1 DEGRADATION PSF MEASUREMENT TECHNIQUES

There are three direct measurement techniques that can frequently be used to determine the system psf.

### 3.1.1 Point Source Measurement

Locate an image of an isolated point source in the degraded output and measure the psf directly by

$$g(x_i,y_i) = \int_{-\infty}^{\infty}\int h(x_i - x_o,\, y_i - y_o) \times \delta(x_o,y_o)\, dx_o\, dy_o = h(x_i,y_i) \ . \quad (10)$$

This method is particularly applicable in astronomical imaging with stellar point sources.

### 3.1.2 Line Source Measurement

Locate an image of an isolated line source in the blurred output and measure the line spread function (lsf) directly by

$$g(x_i,y_i) = \int_{-\infty}^{\infty}\int h(x_i - x_o,\, y_i - y_o)\, \delta(x_o)\, dx_o\, dy_o = \int_{-\infty}^{\infty} h(x_i,y_i - y_o)\, dy_o = h_l(x_i,y_i) \ . \quad (11)$$

In the Fourier domain,

$$FT\{g(x_i,y_i)\} = G(f_x,f_y) = H(f_x,0) \ , \quad (12)$$

where $FT\{\cdot\}$ denotes a two-dimensional Fourier transform. If the psf is known to be circularly symmetric (an isotropic function), $H$ and therefore $h$ are determined. Otherwise we must find the lsf for line sources positioned at varying angles in the image to determine $H$ along several radial lines. Interpolation is used to obtain the transfer function values at rectangular grid locations.

### 3.1.3 Edge Source Measurement

Locate an isolated edge in the degraded image and measure the edge spread function (esf). The derivative of the esf is the lsf and, therefore,

$$H_e(f_x,f_y) = \frac{H_l(f_x,f_y)}{i2\pi f_x} \text{ (edge along } y \text{ axis)} \ . \quad (13)$$

From this result, we can determine the psf as before. Par-target test patterns imaged by the system are frequently used for this technique.

## 3.2 DEGRADATION PSF ESTIMATION TECHNIQUES

The techniques described below are based on homomorphic signal processing (HSP) and cepstral-like techniques to estimate the degrading filter and its parameters.

### 3.2.1 HSP Filter Estimation

The blurred image is subdivided into $N$ regions. This technique requires that the nonzero extent of the psf be small compared to the area of each region. Each region is Fourier transformed to yield

$$G_i(f_x,f_y) \cong H(f_x,f_y)\, F_i(f_x,f_y), \quad (14)$$

where i = 1, 2, . . . , N. The logarithm of the magnitude is taken and the result is summed over the $N$ regions by

$$\sum_{i=1}^{N} ln\, |G_i| \cong N\, ln\, |H| + \sum_{i=1}^{N} ln\, |F_i| \ . \quad (15)$$

The degrading filter is estimated as

$$|H| \cong \exp\left\{\frac{1}{N}\left[\sum_{i=1}^{N} ln|G_i| - \sum_{i=1}^{N} ln\, |F_i|\right]\right\} = \left[\prod_{i=1}^{N} \frac{|G_i|}{|F_i|}\right]^{1/N} \ . \quad (16)$$

[13] A. Rosenfeld and A. C. Kak, *Digital Picture Processing*, 2nd ed., Academic Press, New York (1982).

For this technique to work, the object Fourier transform in each region must either be known or estimated. Another possibility is to assume that for large enough $N$,

$$\frac{1}{N}\sum_{i=1}^{N} ln|F_i| \cong \text{Constant.} \qquad (17)$$

The conditions that must be met to satisfy this last criterion are not well defined and require further investigation.

### 3.2.2 Power Spectral Density Estimation

A related approach treats the object and image as stochastic processes and uses the function power spectral densities (psd) to determine the degrading filter. For linear systems,

$$S_{gg} = |H|^2 S_{ff} , \qquad (18)$$

where $S_{gg}$ and $S_{ff}$ are the psd of the image and object functions, respectively. The blurred image psd can be estimated by the spatial average

$$S_{gg} \cong \frac{1}{N}\sum_{i=1}^{N}|G_i|^2 , \qquad (19)$$

where the assumption is made that the stochastic image process is ergodic. The resulting filter is

$$|H| \cong \left\{\frac{\frac{1}{N}\sum_{i=1}^{N}|G_i|^2}{S_{ff}}\right\}^{1/2} . \qquad (20)$$

The object psd, $S_{ff}$, is either assumed known or is also estimated as a spatial average, and the $|F_i|$, $i = 1, 2, \ldots, N$ are assumed known.

Both of the above estimation techniques lead to an expression for the *magnitude* of the degrading filter; they give no information about the filter phase. For degrading filters that are known a priori to be real and to contain no zero crossings (e.g., Gaussian blur), the filter has been sufficiently determined. If the filter transfer function does contain zero crossings, we may be able to postulate a parametric form for the filter. Estimation techniques can then be used to determine the parameters. Two examples of this parametric estimation method are given below.

### 3.2.3 Parametric Filter Estimation

**3.2.3.1 Linear constant velocity blur.** We consider an imaging system where the only degradation is caused by the linear constant velocity motion of the camera during exposure. Equations 3 and 4 (or others of that form) can be used to determine the LSI psf,

$$h(x,y) = \begin{cases} \frac{1}{v} & 0 \le x\cos\phi + y\sin\phi \le vT \\ & \text{and } y = x\tan\phi \\ 0 & \text{elsewhere.} \end{cases} \qquad (21)$$

The filter transfer function is

$$H(f_x,f_y) = T\,\frac{\sin(\pi fvT)e^{-i\pi fvT}}{\pi fvT} , \qquad (22)$$

where $T$ is the time of exposure, $v$ is the linear velocity, $\phi$ is the angle of motion relative to the $x$ axis, and $f = f_x \cos\phi + f_y \sin\phi$.

This filter clearly has zero crossings and a phase function associated with it. The HSP techniques discussed in Section 3.2 will not work for this degradation and some other method of estimating the filter is required. In particular, we need to estimate the parameters $vT$ and $\phi$. To accomplish this, we compute one-dimensional Fourier transforms of the log magnitude of the blurred image spectrum with respect to both the $f_x$ and $f_y$ frequency axes. The periodic structure of the filter transfer function gives rise to peaks in the two one-dimensional Fourier transforms thus generated at the values $x = vT\sin\phi$ (Fourier transform with respect to $f_x$) and $y = vT\cos\phi$ (Fourier transform with respect to $f_y$). This cepstral-like technique allows us to determine both unknown parameters, $vT$ and $\phi$, which in turn uniquely specify the degrading filter.

**3.2.3.2 Simple defocus aberration.** The degradation arising from a badly defocussed optical system can be modeled as the Airy disk pattern[12]

$$H(f_x, f_y) = \frac{J_1(A\sqrt{f_x^2+f_y^2})}{A\sqrt{f_x^2+f_y^2}} , \qquad (23)$$

where $J_1$ is a Bessel function of the first kind and $A$ is the effective radius of the circular aperture. The log magnitude of the image spectrum after inversion and clipping yields large positive values forming a circle of radius $A$. With this technique, the radius can thus be estimated and the filter determined. Obviously, care must be taken with both parametric estimation methods to avoid logarithms of zero values.

### 3.3 NOISE CONSIDERATIONS

So far, no mention of the effect of noise has been made. In general, the model for the output image will consist of the linearly filtered object plus signal independent noise,

$$g = h * f + n$$

and

$$G = HF + N \,. \tag{24}$$

The introduction of noise into the system will clearly degrade the measured and estimated values for the system filter just derived.

One way to reduce the effect of noise is multiframe averaging. Several frames of the degraded image may be available (as is often the case with video data), and noise reduction can occur by averaging these image frames. Multiframe averaging relies on the assumption that the detector noise is independent from frame to frame to effect a reduction in the noise variance.

The imaging system psf can also be considered to be varying from frame to frame while the object remains unchanged. This is the case when detector camera motion or random turbulent media variations are incorporated in the psf. The summation over $J$ image frames yields

$$g' = h' * f + n' \,, \tag{25}$$

where the new noise term, $n'$, retains the same mean as the original noise but has a variance that is reduced by the factor $1/J$. The new system psf is $h'$ and is the ensemble average of the individual frame psf. If the noise $n'$ has a known mean value and the variance is sufficiently small, degradation measurement or estimation techniques can be applied to the averaged image in Eq. 25 to generate an estimate of $h'$. Restoration can then be carried out on this averaged image to obtain a restored version of the original object.

## 4.0 IMAGE RESTORATION TECHNIQUES

When surveying the image restoration literature, it becomes apparent that a plethora of restoration techniques exists. Each technique is based on particular assumptions about the object and imaging system and is motivated by some form of restoration criteria. A comprehensive discussion of all restoration methods is beyond the scope of this report. Instead, we consider only the most popular and successful methods for both LSI and LSV imaging systems. The strengths and weaknesses of each method are identified and restoration examples are supplied where possible; however, rather than presenting a somewhat long and disjointed list of restoration techniques, we begin with the general concepts that tie these varied methods together.

### 4.1 RESTORATION CRITERIA

Given a degraded image, we would like to use the prior knowledge obtained about the imaging system to perform some operation on the degraded image to effect an "improvement"; i.e., a restored image is generated that in some sense more closely resembles the original object. The choices of criteria used to motivate the improvement and determine the restoration technique fall into four general categories: (a) least squares estimates, (b) equivalent power spectral densities, (c) Bayesian estimates, and (d) ad hoc methods.

Techniques based on least squares estimation treat the original object as a deterministic unknown function. This criterion requires that the squared error between the degraded image and the filtered estimate be minimized,

$$\underset{\hat{f}}{\text{Min}}\{e\} = \underset{\hat{f}}{\text{Min}}\{|g - h * \hat{f}|^2\} \,. \tag{26}$$

Because of the invariant filtering operation, least squares estimation only results in LSI restoration techniques.

The second category is that of equivalent power spectral densities. Techniques that fall into this category treat the object as a stochastic process and generate a restored image whose psd is equal to the known original object psd,

$$S_{\hat{f}\hat{f}} = S_{ff} \ . \tag{27}$$

Bayesian estimation gives rise to a number of estimation criteria depending on the cost function assigned to errors.[14] The stochastic properties of the object and noise are used to develop minimum mean squared error (MMSE), maximum entropy, and maximum a posteriori (MAP) estimates.

In addition to techniques based on these well-defined criteria, others developed on heuristic arguments can also provide good restoration. Application-specific constraints such as non-negativity or second order smoothness can also be introduced to generate various hybrid techniques. Table 2 lists the categories of restoration criteria and the restoration techniques associated with each one. These techniques are discussed in detail in Sections 4.2 and 4.3.

## 4.2 LINEAR SPATIALLY INVARIANT TECHNIQUES

Recall that the LSI imaging system model is

$$g(x_i,y_i) = \int\int_{-\infty}^{\infty} h(x_i - x_o, y_i - y_o) \times f(x_o, y_o)\, dx_o\, dy_o + n(x_i,y_i) \ , \tag{28}$$

**Table 2**
Restoration criteria and techniques.

| Category | Criterion | Techniques: LSI | Techniques: LSV |
|---|---|---|---|
| 1. Least squares estimate | $\text{Min}\{\lvert g - h * \hat{f}\rvert^2\}$ | Inverse filtering | |
| 2. Equivalent power spectral density | $S_{\hat{f}\hat{f}} = S_{ff}$ | Homomorphic filtering<br>Geometric mean filtering ($\alpha = 1/2, \gamma = 1$) | |
| 3. Bayesian estimate | | | |
| Minimum mean square error | $\text{Min}\ E\{\lvert f - \hat{f}\rvert^2\}$ | Wiener filtering<br>Recursive filtering | Analytic continuation |
| Maximum entropy | $\text{Max}\ \{-\hat{f}\ ln\ \hat{f}\}$ | | Maximum entropy filtering |
| Maximum a posteriori | $\text{Max}\ Pr\{\hat{f}\lvert g\}$ | | Maximum a posteriori filtering |
| 4. Ad hoc methods | | Constrained deconvolution<br>Geometric mean filtering ($0 \le \alpha \le 1, \gamma$) | |

[14] H. L. Van Trees, *Detection, Estimation, and Modulation Theory*, Part I, Wiley & Sons, New York (1968).

where the noise is modeled as additive and signal independent. In the Fourier domain, this becomes

$$G(f_x,f_y) = F(f_x,f_y)\,H(f_x,f_y) + N(f_x,f_y) \quad . \quad (29)$$

The subsections below discuss various methods of image restoration applicable to LSI systems. They incorporate techniques that treat the degrading filter, $H$, as deterministic and known, deterministic with unknown parameters, and completely random.

### 4.2.1 Inverse Filtering

The technique of inverse filtering or method of least squares assumes a known (or accurately estimated) deterministic filter transfer function, $H$. It generates a linear restoration filter with psf $m(x,y)$, which satisfies the criterion of minimum squared error,

$$\underset{\hat{f}}{\text{Min}}\{e\} = \underset{\hat{f}}{\text{Min}}\{||g - h * \hat{f}||^2\} \quad . \quad (30)$$

where

$$\hat{f} = m * g \quad . \quad (31)$$

This is easily solved to yield[3]

$$M_{\text{Inverse}} = FT\{m\} = 1/H \quad (32)$$

and

$$\hat{f}_{\text{Inverse}} = FT\{\hat{f}\} = G/H \quad . \quad (33)$$

Equation 33 demonstrates that the inverse filter has severe problems whenever $H = 0$. If $H$ has zeros in the desired image bandwidth, the image cannot be perfectly restored, even in the absence of noise, because of the indeterminate 0/0 ratios that occur. When noise is present, the zeros of $H$ serve to amplify the noise power at these frequencies. If $H$ is reasonably band limited, high-frequency noise power can also be severely increased.

A rough measure of the degradation in signal-to-noise ratio (SNR) from pre- to postrestoration is found by defining a voltage SNR for the degraded image,

$$SNR_g \equiv \frac{||h * f||}{||n||} = \frac{||f||}{||n||} \quad , \quad (34)$$

where the energy conserving property of $h$ has been used[12] and $||\cdot||$ denotes the signal norm.[15] The SNR for the image restored by inverse filtering is defined as

$$SNR_f \equiv \frac{||f||}{||m * n||} < \frac{||f||}{||m||\,||n||} \quad . \quad (35)$$

The ratio of the two SNRs is the degradation in SNR caused by the inverse filtering restoration process,

$$z \equiv \frac{SNR_f}{SNR_g} \leq \frac{1}{||m||} \equiv \frac{1}{||H^{-1}||} \quad , \quad (36)$$

where Parseval's theorem accounts for the last equality. Typical values for $||H^{-1}||$ for real imaging systems are on the order of 100 or higher, demonstrating that the SNR can be severely degraded by a factor of 100 or more when using inverse filtering restoration.

This points out the general ill-conditioned nature of image restoration, which results from the property that small perturbations in the degraded image, $g(x,y)$, can cause large changes in the restored image, $\hat{f}(x,y)$. For example, in the noise-free case,

$$g = h * f$$

$$f = m * g = f \text{ (assuming no 0/0 ratios)}, \quad (37)$$

but when an arbitrarily small amount of noise is added,

$$g = h * f + n_\epsilon$$

$$f = m * g = f + n_\delta \quad , \quad (38)$$

where $n_\delta$ is not necessarily small and can in fact be quite large.

Inverse filtering, however, does have its advantages. It is easy to implement and can be done quickly. It requires only knowledge of the system psf, unlike many other techniques that require knowledge of the noise and object characteristics. In addition, in high-SNR environments it gives restorations with good resolution (providing there are few zeros of $H$ in the image bandwidth). To avoid indeterminate ratios, a pseudoinverse filter can be defined as[12]

$$M_{\text{Pseudoinverse}} = H^+ \equiv \lim_{\gamma \to 0} \frac{H^*}{|H|^2 + \gamma} \quad . \quad (39)$$

[15] L. E. Franks, *Signal Theory*, rev. ed., Dowden & Culver, Stroudsburg, Pa. (1981).

Figure 2 shows an original object function. Figure 3 shows the object after it has been blurred by a low-pass filter and degraded by noise for both a high SNR (33 dB) and a lower SNR (23 dB). The restoration generated by inverse filtering is given in Fig. 4 for the high- and low-SNR cases. As expected, the amplified noise severely degrades the restoration at low image SNRs.

### 4.2.2 Wiener Filtering

The poor noise performance of inverse filtering led to the development of alternate restoration techniques designed to restore degraded images with lower SNRs. This approach treats the original object and noise as statistically uncorrelated random functions and constructs a Bayesian estimate of the object. The system transfer function, $H$, is initially treated as deterministic and known. This method entails finding the LSI restoring filter that minimizes the mean squared error of the resulting estimate. The linear filter that accomplishes this is commonly known as the Wiener filter.[16]

The Wiener filter is derived as follows. The mean squared estimate error is

$$e \equiv E\{|f - \hat{f}|^2\}$$
$$= E\{|f - m * g|^2\} , \qquad (40)$$

**Figure 2** Original object function.[12]

[16] A. Papoulis, *Probability, Random Variables, and Stochastic Processes*, McGraw-Hill, New York (1965).

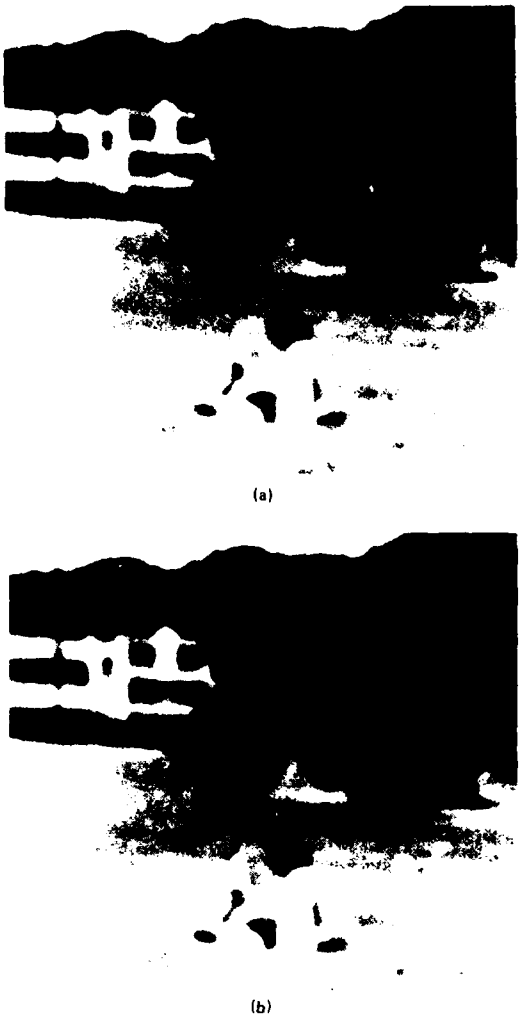


**Figure 3** Object with Gaussian blur and additive noise with (a) SNR = 33 dB and (b) SNR = 23 dB.[12]

where $E\{\cdot\}$ denotes the ensemble average and $m$ is the psf of the Wiener restoration filter. The technique requires that we find the function $m(x,y)$, which minimizes this error. Using the central concept of linear mean square estimation theory, i.e., the orthogonality principle, which states that the error in the estimate must be orthogonal to the data, we obtain

$$E\{[f(x_1,y_1) - m(x_1,y_1) * g(x_1,y_1)]$$
$$g^*(x_2,y_2)\} = 0 \qquad (41)$$

or

$$R_{fg}(\Delta x,\Delta y) = m(\Delta x,\Delta y) * R_{gg}(\Delta x,\Delta y) , \qquad (42)$$

(a)

(b)

**Figure 4** Inverse filtering restoration of Fig. 3 with (a) SNR = 33 dB and (b) SNR = 23 dB.[12]

where $R_{fg}$ and $R_{gg}$ are the cross- and autocorrelation functions of $f$ with $g$ and $g$, respectively. The Fourier transform of Eq. 42 yields

$$S_{fg} = M S_{gg} , \tag{43}$$

where $S_{fg}$ and $S_{gg}$ are the analogous psd. The MMSE Wiener restoration filter is

$$M_{\text{Wiener}} = S_{fg}/S_{gg} . \tag{44}$$

We have implicitly made the assumption that the random object and noise processes are statistically wide-sense stationary. This is frequently not true for real objects, thereby limiting the class of objects for which Wiener filtering truly results in the MMSE estimate. However, we proceed by not only assuming that $f(x,y)$ and $n(x,y)$ are wide-sense stationary, but also constrain them to be uncorrelated. Then

$$M_{\text{Wiener}} = \frac{H^* S_{ff}}{|H|^2 S_{ff} + S_{nn}} , \tag{45}$$

where $S_{nn}$ is the psd of the noise. This may also be written as the product of a simple inverse filter and a modifying filter,

$$M_{\text{Wiener}} = \frac{M_o}{H} = \frac{1}{H}\left[\frac{1}{1 + S_{nn}/|H|^2 S_{ff}}\right] . \tag{46}$$

The modifying filter, $M_o$, is dependent on the stochastic properties of the random object and noise functions. At frequencies where the noise psd is negligible, the Wiener filter behaves as an inverse filter. At frequencies where the noise dominates, the modifying filter provides a weighting factor that adjusts the value of $M$ to be appropriately small. The modifying filter thus supplies a smooth transition between the two noise extremes. Slepian[17] considers the case where the degrading filter, $H$, is also modeled as a random function, and finds that the restoring filter is found by replacing $H^*$ and $|H|^2$ in Eq. 45 by $E\{H^*\}$ and $E\{|H|^2\}$, respectively.

The Wiener filter does not exhibit the singularity problems associated with the inverse filter at the zeros of the system filter $H$. In fact, it is the presence of noise that ensures that the Wiener restoration filter is zero whenever $H$ is zero.

The restoring filter derived in Eq. 46 is the optimum LSI MMSE filter. However, nonlinear filters may exist that yield smaller mean squared errors. In general, the MMSE estimate is given by $\hat{f} = E\{f|g\}$, which may be a nonlinear function of $g$. If $f$ and $n$ are jointly Gaussian and stationary, the MMSE estimate reduces to a simple linear filtering operation and the true MMSE estimate is equal to the LSI MMSE estimate.

[17] D. Slepian, "Linear Least-Squares Filtering of Distorted Images," *J. Opt. Soc. Am.* **57**, 918-922 (1967).

Examples of Wiener filtering restoration of the degraded images in Fig. 3 are shown in Fig. 5. Some resolution is lost in the high-SNR case; however, significant improvement is made in the low-SNR case (cf. Fig. 4).

A parametric version of the MMSE Wiener filter has also been developed. For a specific application, the user can weight the psd ratio in the filter demoninator (Eq. 46) to reflect the degree of importance that should be attached to this stochastic information. This results in the parametric Wiener filter

$$M_{\text{Parametric Wiener}} = \frac{1}{H}\left[\frac{1}{1 + \gamma S_{nn}/|H|^2 S_{ff}}\right], \quad (47)$$

where $\gamma \geq 0$. The parameter $\gamma$ is determined subjectively by the user for a particular image.

(a)

(b)

**Figure 5** Wiener filtering restoration of Fig. 3 with (a) SNR = 33 dB and (b) SNR = 23 dB.[12]

### 4.2.3 Geometric Mean Filtering

We have determined that the simple inverse filter can demonstrate good resolution performance at spatial frequencies where the signal dominates the noise (usually lower frequencies), but is notoriously poor in high-noise regions (usually higher frequencies). The Wiener filter has excellent noise performance but achieves this at the expense of smoothing the restored image by the modifying filter, $M_o$. This can be seen by examining the MMSE restored image in the Fourier domain,

$$\begin{aligned}\hat{F}_{\text{Wiener}} &= M_{\text{Wiener}} G \\ &= \frac{1}{H} M_o \ (HF + N) \\ &= M_o F + \frac{N M_o}{H} \ . \end{aligned} \quad (48)$$

The restored image is no longer a noisy version of the ideal object as in inverse filtering restoration, but a *smoothed* noisy version of $f(x,y)$.

Many applications require better combined noise and resolution performance than either method provides individually. A heuristic technique that attempts to reconcile the trade-off between resolution and noise is geometric mean filtering restoration. The restoration filter is defined as

$$M_{\text{Geometric mean}} = [M_{\text{Inverse}}]^{\alpha} \ [M_{\text{Parametric Wiener}}]^{1-\alpha} \ . \quad (49)$$

The parameters $0 \leq \alpha \leq 1$ and $\gamma \geq 0$ are user defined for a particular image. The user's choice of $\alpha$ thus shifts the emphasis from Wiener to inverse filtering as $\alpha$ varies from zero to one.

### 4.2.4 Constrained Deconvolution

Both Wiener and geometric mean filtering require knowledge of the stochastic properties of the noise and the original object. Constrained deconvolution is simi-

lar to inverse filtering in that it treats the object as an unknown deterministic function.

This technique minimizes the square of a linear constraint on the estimate,

$$\text{Min } \{|c(x,y) * \hat{f}(x,y)|^2\} , \tag{50}$$

subject to a fixed value for the estimate error,

$$e = |g - h * \hat{f}|^2 = E\{n^2\} . \tag{51}$$

The sampled constraint function, $c(x,y)$, is frequently chosen as a second order or higher difference matrix. The second order difference matrix, for example, is defined as the Kronecker product of a tridiagonal matrix $C_1$ with itself, $C = C_1 \times C_1$. The matrix $C_1$ performs the one-dimensional second order differencing operation $[f(x+1) - f(x)] - [f(x) - f(x-1)]$ on the data and is

$$C_1 = \begin{bmatrix} -2 & 1 & & & & & 0 \\ 1 & -2 & 1 & & & & \\ & 1 & -2 & \cdot & & & \\ & & & \cdot & \cdot & \cdot & \\ & & & & \cdot & 1 & \\ & & & & 1 & -2 & 1 \\ 0 & & & & & 1 & -2 \end{bmatrix} .$$

Minimizing the second order difference will prevent the resulting estimate from containing wild oscillations.[12,13]

The method of Lagrange multipliers may be applied to yield the restoration filter

$$M_{\text{constrained deconvolution}} = \frac{H^*}{|H|^2 + \gamma|C|^2} = \frac{1}{H}\left[\frac{1}{1 + \gamma|C|^2/|H|^2}\right] , \tag{52}$$

where $C = FT\{c\}$ and $\gamma$ is related to the Lagrange multiplier. The value of $\gamma$ is adjusted so that the fixed error criterion is satisfied.

Using constrained deconvolution, one can thus choose an estimate error, $E\{n^2\}$ (perhaps determined a posteriori from the degraded image), and generate a restored image that has the desired properties provided by the constraint, $c$. The attractiveness of this technique is that the restored image will have these properties but they will be obtained without detailed knowledge of the object and noise functions' stochastic characteristics.

Figure 6 shows the image restoration achieved by each of the LSI techniques discussed so far for a defocused object with additive high-frequency noise.

### 4.2.5 Homomorphic Deconvolution

Homomorphic image processing for use in a posteriori degradation determination was introduced in Section 3.2. We can proceed with the results of that section to develop a homomorphic restoration filter. This technique is the work of Stockham et al.[11] and Cannon,[18]

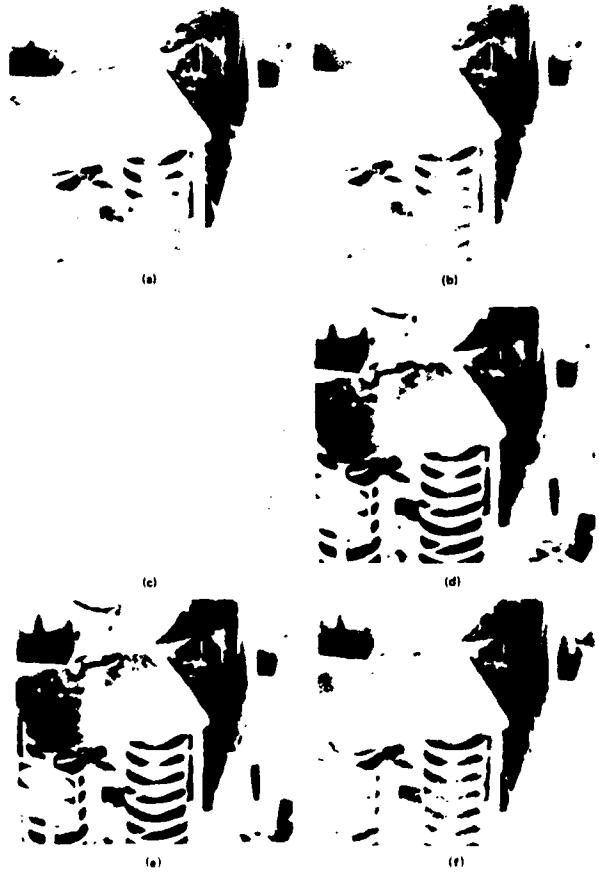

**Figure 6** Restoration by various techniques; (a) original object, (b) original with defocus and high-frequency noise, (c) inverse filtering restoration, (d) Wiener filtering restoration, (e) geometric mean filtering restoration $\alpha = \frac{1}{2}, \gamma = 1$, (f) constrained deconvolution restoration using $C$ = second difference.[12]

[18]M. Cannon, "Blind Deconvolution of Spatially Invariant Blurs with Phase," *IEEE Trans. Acoust. Speech Signal Process.* **24**, 58-63 (1976).

and is also known as blind deconvolution. It is unique among the restoration techniques discussed so far because it does not assume that the system degradation filter $H$ is known.

As in Section 3.2, we subdivide the degraded image into $N$ regions and Fourier transform each region. The psd of the blurred image is estimated by (ergodic assumption)

$$S_{gg} \cong \frac{1}{N} \sum_{i=1}^{N} |G_i|^2 \ . \tag{53}$$

The image estimate in the Fourier domain is

$$\hat{F} = MG \ , \tag{54}$$

where $M$ is the homomorphic restoration filter yet to be determined. The psd of the estimate is therefore

$$S_{\hat{f}\hat{f}} = |M|^2 \, S_{gg} \ . \tag{55}$$

The restoration criterion (see Table 2) for this technique is to equate the original object and estimate image psd, i.e.,

$$S_{\hat{f}\hat{f}} = S_{ff}$$

or

$$|M|^2 S_{gg} = S_{ff} \ , \tag{56}$$

which yields

$$|M_{\text{Homomorphic deconvolution}}| = [S_{ff}/S_{gg}]^{1/2} \ . \tag{57}$$

Here, $S_{ff}$ is assumed known or may be estimated from an undegraded image with structure similar to that of the original object.

The homomorphic restoration filter derived is the reciprocal of the degrading filter estimated by Eq. 20. However, it is not a simple inverse filter as the following argument illustrates. If the object and noise are wide-sense stationary and uncorrelated random processes, we know

$$S_{gg} = |H|^2 \, S_{ff} + S_{nn} \ , \tag{58}$$

where the noise is assumed to be additive with psd $S_{nn}$. Then,

$$|M| = \left[ \frac{S_{ff}}{|H|^2 \, S_{ff} + S_{nn}} \right]^{1/2} , \tag{59}$$

which is the magnitude of the geometric mean filter with $\alpha = 1/2$ and $\gamma = 1$,

$$|M_{\text{Homomorphic deconvolution}}| = |M_{\text{Geometric mean, } \alpha = 1/2, \, \gamma = 1}| \ . \tag{60}$$

Thus the magnitude of the homomorphic filter is the magnitude of the geometric mean of the inverse filter and the Wiener filter for wide-sense stationary and uncorrelated object and noise. This exciting result is obtained *without* knowledge of the noise psd or the degradation filter $H$. The only information required is an estimate of the object psd ($S_{ff}$) and the degraded image itself. However, this technique yields only the magnitude of the restoring filter. Unless the degrading filter is known to contain no zero crossings (e.g., Gaussian blur), additional methods such as those described in Section 3.2 must be used to estimate the restoration filter phase. Figure 7 shows the effectiveness of this technique on the blurred images in Fig. 3.

#### 4.2.6 Recursive Filtering

Recursive filtering is a specialized restoration technique that assumes that the original object is corrupted only by additive white noise. The degradation psf of the imaging system reduces to $h(x,y) = \delta(x,y)$, a two-dimemsional dirac function, for this technique and

$$g(x,y) = f(x,y) + n(x,y) \ . \tag{61}$$

The object $f(x,y)$ is modeled as a two-dimensional wide-sense Markov process. Recall that for a one-dimensional $N$th order Markov process, the value of the function at a given sample location is dependent only on the values of the preceding $N$ samples. A two-dimensional $(N,M)$th order Markov process stipulates that the sample value at a given location is dependent on the values of the preceding $N$ by $M$ block of samples,

$$Pr\{f(x+1, y+1) \mid f(i,j) \text{ for all } i \le x, j \le y\} = Pr\{f(x+1, y+1) \mid f(i,j) \text{ for } x - N < i \le x, \ y - M < j \le y\} \ . \tag{62}$$

(a)

(b)

**Figure 7** Homomorphic deconvolution restoration of Fig. 3 with (a) SNR = 33 dB and (b) SNR = 23 dB.[12]

In image restoration applications, this technique is frequently used assuming that the original object is a simple two-dimensional first order Markov process. The linear estimate of $f(x+1, y+1)$ has been found to be[13]

$$\hat{f}(x+1,y+1) = a_1\hat{f}(x+1,y) + a_2\hat{f}(x,y+1) + a_3\hat{f}(x,y) + a_4 g(x,y) \quad . \quad (63)$$

The coefficients $\{a_i\}$ are found by minimizing the mean squared error for the estimate $\hat{f}(x,y)$ and are

$$a_1 = \rho_x \quad (64a)$$

$$a_2 = \rho_y \quad (64b)$$

$$a_3 = \rho_x\rho_y + a_4 \quad (64c)$$

$$a_4 = \frac{\rho_x C(1,0) + \rho_y C(0,1) - \rho_x\rho_y C(0,0)}{C(0,0) + \sigma_n^2} \quad , \quad (64d)$$

where $C$ is the object and estimate cross covariance,

$$C(\Delta x, \Delta y) = E\{[f(x,y) - \hat{f}(x,y)]$$

$$[f(x+\Delta x, y+\Delta y) - \hat{f}(x+\Delta x, y+\Delta y)]\} \quad , (65)$$

and $\sigma_n^2$ is the variance of the white noise.

For Eq. 64, the autocorrelation function of the object is postulated to be spatially separable and equal to

$$R_{ff}(\Delta x, \Delta y) = \rho_x^{|\Delta x|}\,\rho_y^{|\Delta y|} \quad . \quad (66)$$

Recursive filtering is substantially different from the other LSI restoration techniques previously described because it operates in the spatial and not the Fourier domain. Since the point spread matrix of the filter is of limited non-zero extent (four-element array for a first order Markov process), the spatial convolution can be implemented quickly on the computer. A distinct disadvantage of this approach is that the adjacent sample correlations must be assumed constant throughout the entire image to yield a spatially invariant restoration filter. This is clearly not realistic for most images, which may contain, for example, regions of essentially constant background ($\rho_x = \rho_y \cong 1$) in addition to regions of rapidly varying intensities ($\rho_x, \rho_y << 1$).

This gives rise to the development of the spatially variant restoration technique of regional recursive filtering. Each regional filter may be applied to areas of the image that have similar spatial correlation properties. Segmentation of the image into these regions and the determination of the individual recursive filters clearly add to the complexity of the technique. Regional recursive filtering also creates artifacts at the region boundaries that must be smoothed by additional processing.

## 4.3 LINEAR SPATIALLY VARIANT TECHNIQUES

Section 4.2 outlined those restoration techniques applicable to LSI systems. Because the imaging system was modeled as spatially invariant, the powerful theory of Fourier domain analysis could be used. However, real imaging systems are seldom spatially invariant and are more appropriately modeled as

$$g(x_i,y_i) = \int_{-\infty}^{\infty}\int h(x_i,y_i,x_o,y_o) \times f(x_o,y_o)\, dx_o\, dy_o + n(x_i,y_i) , \quad (67)$$

where the system psf is a function of both the object and image coordinates.

The simple solutions afforded previously by Fourier analysis techniques no longer apply because of the spatial variance of the system psf. Restoration techniques for LSV systems are, therefore, fewer in number and more difficult to implement.

### 4.3.1 Isoplanatic Patches

The simplest approach to LSV restoration is to divide the blurred image into regions or isoplanatic patches. In each isoplanatic patch the spatially invariant assumption is approximately valid so that we may model the system as piecewise LSI,

$$g_j(x_i,y_i) \cong \int_{x}\int h_j(x_i - x_o,\, y_i - y_o) \times f(x_o,y_o)\, dx_o\, dy_o , \quad (68)$$

for $(x_i,y_i)$ in the $j$th isoplanatic patch. Any of the previously derived spatially invariant restoration techniques can then be applied to the individual patches. As with regional recursive filtering, postprocessing is usually required to reduce artifacts generated at the restored image isoplanatic region boundaries.

### 4.3.2 Coordinate Distortion Method

A novel approach to spatially variant image restoration developed by Sawchuk[19] and Robbins and Huang[6] hinges on finding a nonlinear coordinate transformation that maps the imaging system to a linear spatially invariant domain. An LSI technique can then be used to restore the image in this new domain, and an inverse coordinate transformation of the result yields the restored image in the original coordinate system.

The application of this approach is limited to those LSV systems that are decomposable into the general form shown in Fig. 8. However, the effects of many forms of spatially variant image degradation can be described by this decomposition. The applicability of this coordinate distortion technique for restoring images degraded by certain types of camera motion[19,20] and by the optical aberrations of astigmatism and curvature of field[8] has also been shown.

For example, a simple rotation of the camera about the optical axis yields the LSV result

$$g(x_i,y_i) = \int \frac{f(x_o,y_o)}{\omega\sqrt{x_o^2 + y_o^2}}\, ds_o \quad (69)$$

along $x_o^2 + y_o^2 = x_i^2 + y_i^2$ .

The limits of integration are from

$$x_o = x_i \qquad x_o = x_i \cos \omega T + y_i \sin \omega T$$

to

$$y_o = y_i \qquad y_o = x_i \sin \omega T + y_i \cos \omega T .$$

Here,

$\omega$ = constant angular rotational velocity,
$T$ = time of photographic exposure,
$ds_o$ = differential path element,

and $\omega T$ is constrained to be less than $2\pi$ radians (overall camera motion must be less than one full rotation).

The imaging system is otherwise considered to be perfect, and no noise is introduced for this simple example. By transforming to polar coordinates $(r, \theta)$, we obtain

$$\begin{aligned} g(r_i,\theta_i) &= \int_{\theta_o=\theta_i}^{\theta_o=\theta_i+\omega T} \frac{f(r_o,\theta_o)}{\omega}\, d\theta_o \\ &= \int_{\theta=-\omega T}^{0} \frac{f(r_o,\theta_i-\theta)}{\omega}\, d\theta \\ &= \int_{-\infty}^{\infty} f(r_o,\theta_i-\theta)\, h(\theta)\, d\theta , \end{aligned} \quad (70)$$

[19] A. A. Sawchuk, "Space-Variant Image Motion Degradation and Restoration," *Proc. IEEE* **60**, 854-861 (1972).
[20] A. A. Sawchuk, "Space-Variant System Analysis of Image Motion," J. Opt. Soc. Am. **63**, 1052-1063, (1973).

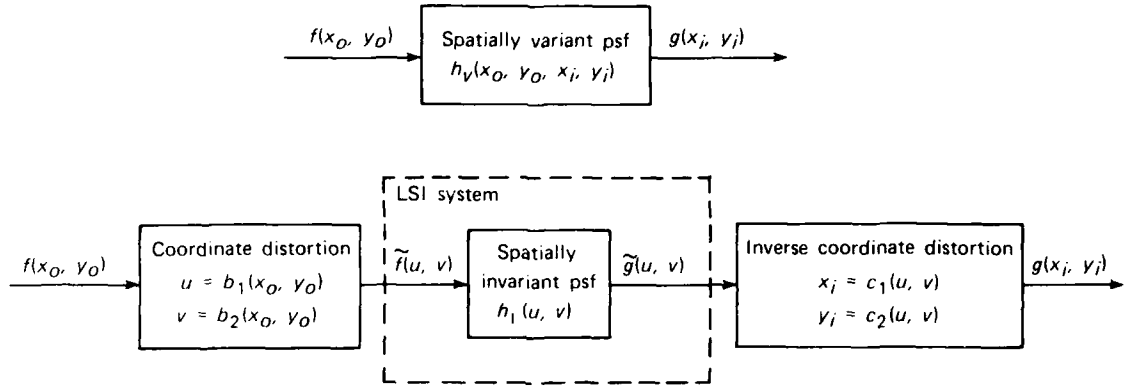


**Figure 8** LSV coordinate distortion restoration.

where $h(\theta) = (1/\omega)$ for $-\omega T \leq \theta \leq 0$. The system is spatially invariant with respect to the new coordinate domain. An LSI technique can now be used to restore the image before transforming back to Cartesian coordinates. Figure 9 shows the usefulness of this technique for an image blurred by camera rotation. The LSI technique used to develop the restored image in Fig. 9c was a simple inverse filter.

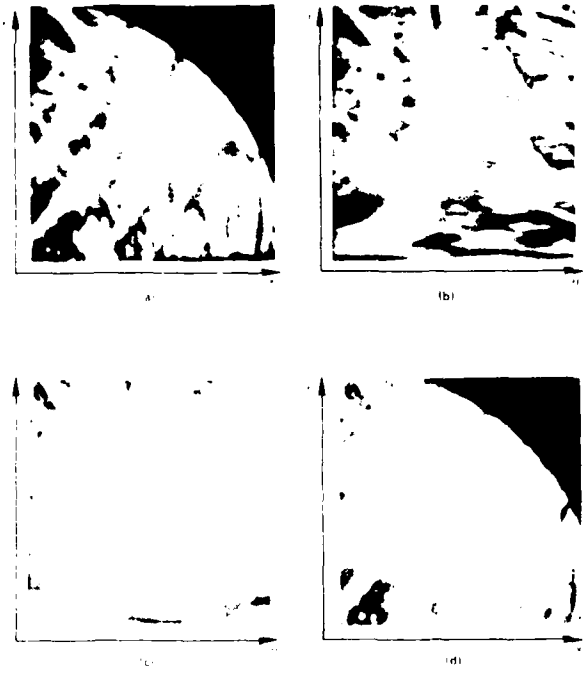

**Figure 9** Coordinate distortion restoration of rotational blur: (a) rotationally blurred object, (b) blurred object transformed to polar coordinates, (c) LSI restoration of transformed object, (d) restored image transformed back to Cartesian coordinates.[12]

The drawbacks of this technique stem from: a) being able to define the coordinate transformation for a given LSI image restoration application; and b) determining the object and noise stochastic properties in the new coordinate system. The latter point is relevant when LSI estimation is used to restore the degraded image. For example, we cannot expect that minimizing the mean squared estimate error in the transformed domain will necessarily minimize the mean squared error in the original coordinate system. However, for specific applications (e.g., camera motion and aberration correction), this technique may be quite useful.

### 4.3.3 Maximum A Posteriori Restoration

Maximum a posteriori (MAP) restoration is a nonlinear iterative technique that, in its most general form, is applicable to spatially variant imaging systems. We describe the technique for a discrete imaging system where the sampled image, object, and noise data are lexicographically ordered into one-dimensional vectors,

$$\mathbf{g} = [H]\,\mathbf{f} + \mathbf{n}\,, \tag{71}$$

and $H$ is a two-dimensional matrix representing the effects of the spatially variant system psf.

The MAP estimate of the vector $\mathbf{f}$ is given by

$$\max_{\hat{\mathbf{f}}} \{Pr(\hat{\mathbf{f}}|\mathbf{g})\} \Big|_{\hat{\mathbf{f}} = \hat{\mathbf{f}}_{MAP}}\,. \tag{72}$$

Bayes's rule states

$$Pr\{\mathbf{f}|\mathbf{g}\} = \frac{Pr\{\mathbf{g}|\mathbf{f}\}\ Pr\{\mathbf{f}\}}{Pr\{\mathbf{g}\}}\,, \tag{73}$$

which is the expression we need to maximize with respect to $\mathbf{f}$. If the original object and noise can be modeled as multivariate Gaussian processes, i.e.,

$$Pr\{\mathbf{f}\} = A_1 \exp\left\{-\frac{1}{2}(\mathbf{f}-\bar{\mathbf{f}})^T [C_f]^{-1} (\mathbf{f}-\bar{\mathbf{f}})\right\}, \quad (74)$$

$$Pr\{\mathbf{n}\} = A_2 \exp\left\{-\frac{1}{2}\mathbf{n}^T [C_n]^{-1} \mathbf{n}\right\}, \quad (75)$$

where $[C_f]$ and $[C_n]$ are the object and noise covariance matrices, the MAP estimate is found by iteratively solving

$$\hat{\mathbf{f}}_{MAP} = \bar{\mathbf{f}} + [C_f]H^T[C_n]^{-1}[\mathbf{g} - H\hat{\mathbf{f}}_{MAP}] \quad (76)$$

for $\hat{\mathbf{f}}_{MAP}$. Although the multivariate Gaussian assumption may seem overly restrictive at first, it gives a reasonable model for many images. The underlying structure of the object can be modeled in the mean vector $\bar{\mathbf{f}}$, with the finer structure described by Gaussian variations about this mean vector. This may be a more realistic model than that obtained by assuming a wide-sense stationary object. Recall that the stationarity assumption requires that every element in the mean vector $\bar{\mathbf{f}}$ be equal to the same constant value (as in Wiener, geometric mean, and recursive filtering).

The MAP restoration technique requires a great deal of prior knowledge as Eq. 76 demonstrates. The object and noise stochastic properties, as well as the imaging system degradation effects, must be specified. The iterative nature of this technique also makes it computationally expensive and convergence is not always guaranteed. However, MAP restoration has been used successfully in certain applications[21] and can be extended to nonlinear spatially variant imaging systems as well.

### 4.3.4 Superresolution Techniques

The limit of attainable image resolution using the definition derived from the Rayleigh criterion[2] is determined by the cutoff spatial frequency of the imaging system. Even with the best possible restoration technique, object information outside of the system bandwidth is lost; we would expect a minimum resolvable spatial element corresponding to the inverse of the system cutoff frequency. However, if certain conditions can be placed on the object, it is possible (in theory, at least) to determine the object spectrum outside of the system bandwidth. The restored image would then achieve the property of spatial superresolution—resolution beyond the limit imposed by the system cutoff frequency. Two techniques that have this property are maximum entropy restoration[4,5] and the method of analytic continuation.[22,23] Unfortunately, both techniques require extremely high SNRs to achieve superresolution.

Maximum entropy restoration is based on modeling the original object vector $\mathbf{f}$ (suitably normalized) as a probability density function (pdf). This condition guarantees positive values for the restored image vector $\hat{\mathbf{f}}$. A derivation based on multinomial pdf (e.g., see Refs. 4 and 5) yields

$$\hat{\mathbf{f}}_{\text{Max entropy}} = \exp\{-\mathbf{1} - 2\lambda[H^*]^T (\mathbf{g} - H\hat{\mathbf{f}}_{\text{Max entropy}})\}, \quad (77)$$

where the additional constraint $\|\mathbf{g} - H\mathbf{f}\|^2 = \|\mathbf{n}\|^2$ has been incorporated using the method of Lagrange multipliers. Maximum entropy, like MAP restoration, is a nonlinear iterative technique. The estimate derived is intrinsically not band limited and thus superresolution results in high-SNR cases.

The method of analytic continuation is based on an eigenfunction expansion of the spatially limited object whose Fourier spectrum is known only in the system bandwidth. Prolate spheroidal wave functions have the interesting properties of being a) orthonormal on the real line and b) a complete orthogonal basis for the set of functions band limited to a specified bandwidth. If the imaging system is modeled as a spatially separable system defined by a rectangular aperture, the dual characteristics of the prolate spheroidal wave functions (pswf) lead to a non-band-limited estimate for the original object (see Refs. 22 and 23 for details). However, image SNRs on the order of 30 dB or more are required for analytic continuation to result in useful restoration. In addition, the pswf and the resulting image estimate are difficult to compute, which further limits the usefulness of this technique.

[21] B. R. Hunt, "Digital Image Processing," *Proc. IEEE* **63**, 693-708 (1975).

[22] C. K. Rushforth and R. W. Harris, "Restoration, Resolution, and Noise," *J. Opt. Soc. Am.* **58**, 539-545 (1968).

[23] C. L. Rino, "Bandlimited Image Restoration by Linear Mean-Square Estimation," *J. Opt. Soc. Am.* **59**, 547-553 (1969).

# 5.0 COMPARISON OF RESTORATION TECHNIQUES

The restoration techniques discussed in Sections 4.2 and 4.3 are summarized in Table 3. As the second column of the table demonstrates, the LSI restoration filters appear to be strikingly similar. We have seen that these filters can even be equivalent under certain conditions; homomorphic deconvolution is equivalent to geometric mean filtering if the object and noise are uncorrelated and wide-sense stationary. Also, constrained deconvolution is equivalent to parametric Wiener filtering if the constraint is chosen such that $C = S_{nn}/S_{ff}$. Even nonlinear maximum entropy restoration can be related to a simpler LSI technique. If a linear approximation to the exponential in Eq. 77 is made and $[H]$ is assumed LSI, discrete pseudoinverse filtering restoration results.[12]

Given the similarities between the restoration filters, how does a user choose one technique over another for a particular application? There are important factors that differentiate the image restoration techniques and act as guidelines for application, including the following:

1. The restored image quality or perceptibility to a human observer is an important performance factor that depends on the restoration technique used.
2. The noise performance of a given technique is a function of the overall image SNR as well as the type and severity of the image degradation.
3. Each technique requires certain a priori knowledge and imposes restrictive assumptions on the imaging system model which limit its application.
4. The feasibility of using a restoration technique for a specific application is often determined by the length of time required to implement the algorithm.

Most of these factors are delineated in Table 3. One other factor that influences the performance of the restoration technique is the nature of the system noise. The noise type, auto- and crosscorrelation properties, and action on the system (additive, multiplicative) will also effect the performance. This effect is difficult to characterize other than by stating that we would, of course, expect reduced restoration performance for techniques with restrictive system assumptions that do not fit the application.

A quick (albeit coarse) comparison of the most commonly used restoration techniques for the four performance criteria defined above is given in Table 4.[21,24] That the visual quality of the MAP, homomorphic, and geometric mean filters is, in general, better than Wiener filtering may be surprising at first, since Wiener filtering supplies the MMSE estimate. However, Wiener filtering yields the MMSE estimate for wide-sense stationary object and noise functions. This assumption is seldom true for real images. Also, the Wiener filter trades improved noise performance for reduced image resolution. As studies of the human visual system have shown,[25] human observers are usually willing to accept some additional image noise in order to gain improved resolution.

The noise performance of the techniques shows that inverse filtering, as expected, provides unsatisfactory restoration in low-SNR environments. This technique is especially sensitive to high-frequency noise. The other restoration filters listed in Table 4 work well in noisy environments. As the SNR increases, however, the restoration achieved by any of the techniques converges to that of simple inverse filtering.

The degree of information necessary for each technique varies widely for the restoration methods listed. Homomorphic deconvolution requires the least amount of a priori knowledge while Wiener, geometric mean, and MAP filtering require detailed information about the imaging degradation and stochastic properties of the object and noise. The degree of information needed for inverse filtering and constrained deconvolution falls between these two extremes.

Often, the most important factor in choosing a restoration technique is its computational complexity. If large amounts of image data need to be processed quickly and cost effectively, it would be implausible to use an iterative algorithm (without guaranteed convergence) like MAP restoration. Even the partitioning required to compute and apply the homomorphic filter may take too much time for such an application. Inverse, Wiener, geometric mean, and constrained deconvolution filtering have moderately fast implementations using two-dimensional fast Fourier transform (FFT) algorithms. Wiener filtering has an additional advantage; the restoration filtering can be performed in any unitary transform domain. Fourier, Hadamard, identity, or Karhunen-Loeve transform processing is chosen depending on which technique yields the fastest implementation for

[24] T. M. Cannon, H. J. Trussell, and B. R. Hunt, "Comparison of Image Restoration Methods," *Appl. Opt.* **17**, 3384–3390 (1978).

[25] T. G. Stockham, Jr., "Image Processing in the Context of a Visual Model," *Proc. IEEE* **60**, 828–842 (1972).

**Table 3**
Summary of image restoration techniques.

| Restoration technique | Restoring filter | Restoration criterion | A priori knowledge and assumptions | Performance advantages | Disadvantages | Restoring filter variations |
|---|---|---|---|---|---|---|
| Inverse filtering | $M = \frac{1}{H}$ | Min$\|g - h*\hat{f}\|^2$ | LSI system<br>H known | Computational simplicity | Amplifies high-frequency noise<br>Indeterminate when $H = 0$ | Pseudoinverse $M = H^+ = \lim_{\gamma \to 0}\left[\frac{H^*}{\gamma + \|H\|^2}\right]$ |
| Wiener filtering | $M = \frac{1}{H}\left[1 + \frac{S_{nn}}{\|H\|^2 S_{ff}}\right]^{-1}$ | Min $E\{\|f - \hat{f}\|^2\}$ | LSI system<br>$H$, $S_{nn}$, $S_{ff}$ known<br>$n$, $f$ stationary | Optimum linear MSE estimate<br>Good noise performance<br>$M = 0$ when $H = 0$ | Stationary $f$ assumption unrealistic<br>Restored image is smoothed | Parametric Wiener $M = \frac{1}{H}\left[1 + \gamma \frac{S_{nn}}{\|H\|^2 S_{ff}}\right]^{-1}$ |
| Geometric mean filtering | $M = \frac{1}{H}\left[1 + \gamma \frac{S_{nn}}{\|H\|^2 S_{ff}}\right]^{-\alpha}$ | User defined | LSI system<br>$H$, $S_{nn}$, $S_{ff}$ known<br>$n$ $f$ stationary | Combines good low-frequency restoration of inverse filtering with high-frequency noise performance of Wiener filtering<br>User tailored for each image | Stationary $f$ assumption unrealistic<br>Iterative and subjective method to find parameters $\gamma$, $\alpha$ | True geometric mean, $\alpha = \frac{1}{2}$, $\gamma = 1$<br>Inverse filter, $\alpha = 1$<br>Parametric Wiener, $\alpha = 0$ |
| Constrained deconvolution | $M = \frac{1}{H}\left[1 + \frac{\gamma C^2}{H^2}\right]^{-1}$ | Min $\|c*\hat{f}\|^2$ subject to $\|g - h*\hat{f}\|^2 = \sigma_n^2$ | LSI system<br>$H$, $\sigma_n^2$ known<br>$C$ user defined | User-defined constraint generates desired restoration without knowledge of $S_{ff}$, $S_{nn}$ | Iterative method to find $\gamma$<br>Restoration more noise sensitive than Wiener filtering | Finite second degree difference matrix $\{c(i,j)\}$<br>Human visual response model $\{c(i,j)\}$ |
| Homomorphic deconvolution | $M = \left[\frac{N S_{ff}}{\sum_{i,j} \|G_{ij}\|^2}\right]$ | $S_{ff} = S_{ff}$ | LSI system<br>$S_{ff}$ known<br>Extent of $H <$ area of partition block<br>Ergodic $g$ | No knowledge of $H$ required<br>Good noise performance | Magnitude-only restoration filter requires additional processing to determine filter phase<br>Computationally complex | Equivalent to geometric mean with $\alpha = \frac{1}{2}$, $\gamma = 1$ for stationary $f$, $n$ |
| Recursive filtering | — | Min $E\{\|f - \hat{f}\|^2\}$ | Ideal LSI imaging system<br>White additive noise<br>$f(x,y)$ is $(N,M)$th order wide-sense Markov<br>$R_{ff}$ and $C_{ff}$ known | Quick filter implementation | Restrictive and unrealistic assumptions | LSV regional recursive filtering |
| Isoplanatic patch filtering | Any LSI filter | — | LSV system is piecewise LSI plus LSI technique assumptions | Straightforward implementation | Computationally expensive | — |
| Coordinate distortion method | Any LSI filter | — | LSV system described as LSI after known coordinate transformation plus LSI technique assumptions | Fast LSV restoration achieved when coordinate transformation known | Only works for certain decomposable LSV systems (Fig. 8) | — |
| MAP[a] restoration | — | Max $Pr(\hat{f}\|g)$ | LSV system<br>$f$ and $g$ multivariate Gaussian processes<br>$[H]$, $\bar{f}$, $[C_f]$, $[C_n]$ known | Visually pleasing restoration | Iterative technique<br>Convergence not guaranteed | — |
| Maximum[b] entropy | — | Max $\{-\hat{f} \ln \hat{f}\}$ | LSV system<br>$f$, $\hat{f}$ non-negative<br>$[H]$, $\sigma_n^2$ known | Visually pleasing restoration<br>Superresolution | Iterative technique<br>Convergence not guaranteed<br>Very susceptible to noise | |
| Analytic[c] continuation | — | Min $E\{\|f - \hat{f}\|^2\}$ | LSV system<br>$f$ analytic and band-limited to square band region<br>Prolate spheroidal wave functions known | Superresolution | Computationally expensive<br>Requires very high SNR (> 30 dB) | — |

[a] For details regarding this technique, see Section 4.2.6
[b] See Section 4.3.3
[c] See Section 4.3.4

**Table 4**
Comparison of restoration techniques.

| | Visual quality (moderate SNR) | Noise performance | Degree of required a priori knowledge | Computational complexity |
|---|---|---|---|---|
| Inverse filtering | Fair | Poor | Low | Low |
| Wiener filtering | Good | Good | High | Moderate |
| Geometric mean filtering | Very good | Good | High | Moderate |
| Constrained deconvolution | Good | Fair | Moderate | Moderate |
| Homomorphic deconvolution | Very good | Good | Low | High |
| MAP restoration | Very good | Good | High | Very high |

the particular image.[26] (See Ref. 12 for restoration algorithms and additional insight on their implementation.)

Ultimately, the choice of restoration technique is determined by the particulars of the application. What kind of visual quality is required? A restored image that will be subsequently processed by additional software for classification/detection purposes will not necessarily require the same degree of visual quality as one that will be presented to a human observer. What is the system SNR and how severe is the degradation? If the system consistently operates at high SNRs, simple inverse filtering may suffice. What kind of prior knowledge is available? If little information about the system is known or estimable, homomorphic deconvolution may be the most attractive technique. However, the user must remember the assumptions couched in this method: the non-zero extent of $H$ is less than the partition size and $H$ is real and non-negative.

And finally, what are the computational considerations for the particular application? Are there reels of data or a single image to restore? Is the data stored and processed in an image processing laboratory or must restoration be accomplished in close to real time? For very fast restoration applications, the format of the image data can further influence the choice of restoring technique. For example, video image data received one scan line at a time lends itself to techniques that can be implemented by one-dimensional line processing. Even though faster two-dimensional FFT algorithms exist that operate on a two-dimensional extension of the one-dimensional Cooley-Tukey butterfly operation,[27] most two-dimensional FFT algorithms are performed by sequential one-dimensional FFT computations. This makes techniques such as inverse, Weiner, geometric mean, and constrained deconvolution filtering especially applicable to scanned imagery.

[26]W. K. Pratt, "Generalized Wiener Filtering Computation Techniques," *IEEE Trans. Comp.* **C-21**, 636-641 (1972).

[27]D. B. Harris, J. H. McClellan, D. S. K. Chan, and H. W. Schuessler, "Vector Radix Fast Fourier Transform," IEEE Conf. on Acoustics, Speech, and Signal Processing, Hartford, Conn. (May 9-11, 1977).

# 6.0 CONCLUSIONS

Although the techniques discussed above represent those most frequently used, they are only a subset of the image restoration techniques that have been developed. Some additional methods are maximum likelihood, maximum weighted Burg entropy, and even minimum entropy.[12] Frieden[28] unifies Bayesian estimate methods under a general theory of maximum physical likelihood (note, however, that Frieden's definition of maximum likelihood differs from convention). Several nonlinear and linear recursive restoration techniques are studied in another publication by Meinel.[29]

With the exception of maximum entropy and MAP restoration, the techniques in Section 4.0 do not guarantee non-negative values for the restored image, $\hat{f}$. If the optical intensity of the object is measured by the function $f$ (i.e., $f \geq 0$), we would prefer that the restored image be non-negative also ($\hat{f} \geq 0$). This can be done by adding a positivity constraint to any restoration criterion. Unfortunately, this usually does not lead to a closed form expression for the restored image and requires computationally intensive nonlinear programming to obtain a solution.

New image restoration techniques can be developed simply by defining new restoration criteria. Most current techniques are based on criteria that generate visually pleasing restorations. However, if the restored image is subsequently processed by additional software rather than presented to a human observer, it may be possible to develop new techniques that optimize the performance of this postrestoration processing. One application where this may prove profitable is in the area of automatic scene detection and classification. Potentially, one could develop a restoration technique based on a criterion that would be tailored to give maximum probability of detection and correct classification of the resultant restored image scenes.

[28] B. R. Frieden, "Unified Theory for Estimating Frequency-of-Occurrence Laws and Optical Objects," *J. Opt. Soc. Am.* 73, 927-938, (1983).

[29] E. S. Meinel, "Origins of Linear and Nonlinear Recursive Restoration Algorithms," *J. Opt. Soc. Am.* 3, 787-799 (1986).

## REFERENCES

[1]R. E. Hufnagel and N. R. Stanley, "Modulation Transfer Function Associated with Image Transmission through Turbulent Media," *J. Opt. Soc. Am.* **54**, 52-61 (1964).

[2]J. W. Goodman, *Introduction to Fourier Optics,* McGraw-Hill, San Francisco (1968).

[3]T. S. Huang, W. F. Schreiber, and O. J. Tretiak, "Image Processing," *Proc. IEEE* **59**, 1586-1609 (1971).

[4]B. R. Frieden, "Restoring with Maximum Likelihood and Maximum Entropy," *J. Opt. Soc. Am.* **62**, 511-518 (1972).

[5]B. R. Frieden and J. J. Burke, "Restoring with Maximum Entropy II: Superresolution of Photographs of Diffraction-Blurred Impulses," *J. Opt. Soc. Am.* **62**, 1202-1210 (1972).

[6]G. M. Robbins and T. S. Huang, "Inverse Filtering for Linear Shift-Variant Imaging Systems," *Proc. IEEE* **60**, 862-872 (1972).

[7]A. A. Sawchuk, "Space-Variant Image Restoration by Coordinate Transformations," *J. Opt. Soc. Am.* **64**, 138-144 (1974).

[8]A. A. Sawchuk and M. J. Peyrovian, "Restoration of Astigmatism and Curvature of Field," *J. Opt. Soc. Am.* **65**, 712-715 (1975).

[9]T. J. Harris, "Evaluation of Environmental Optical Effects on High Speed Hemispherical Domes Using a Ray Trace Model," JHU/APL F1F(2)86-U-066 (Apr 1986).

[10]D. A. O'Handley and W. B. Green, "Recent Developments in Digital Image Processing at the Image Processing Laboratory at the Jet Propulsion Laboratory," *Proc. IEEE* **60**, 821-828 (1972).

[11]T. G. Stockham, T. M. Cannon, and R. B. Ingebretsen, "Blind Deconvolution through Digital Signal Processing," Proc. IEEE **63**, 678-692 (1975).

[12]H. C. Andrews and B. R. Hunt, *Digital Image Restoration,* Prentice-Hall, Englewood Cliffs, N.J. (1977).

[13]A. Rosenfeld and A. C. Kak, *Digital Picture Processing*, 2nd ed., Academic Press, New York (1982).

[14]H. L. Van Trees, *Detection, Estimation, and Modulation Theory*, Part I, Wiley & Sons, New York (1968).

[15]L. E. Franks, *Signal Theory,* rev. ed., Dowden & Culver, Stroudsburg, Pa. (1981).

[16]A. Papoulis, *Probability, Random Variables, and Stochastic Processes*, McGraw-Hill, New York (1965).

[17]D. Slepian, "Linear Least-Squares Filtering of Distorted Images," *J. Opt. Soc. Am.* **57**, 918-922 (1967).

[18]M. Cannon, "Blind Deconvolution of Spatially Invariant Blurs with Phase," *IEEE Trans. Acoust. Speech Signal Process.* **24**, 58-63 (1976).

[19]A. A. Sawchuk, "Space-Variant Image Motion Degradation and Restoration," *Proc. IEEE* **60**, 854-861 (1972).

[20]A. A. Sawchuk, "Space-Variant System Analysis of Image Motion," J. Opt. Soc. Am. **63**, 1052-1063, (1973).

[21]B. R. Hunt, "Digital Image Processing," *Proc. IEEE* **63**, 693-708 (1975).

[22]C. K. Rushforth and R. W. Harris, "Restoration, Resolution, and Noise," *J. Opt. Soc. Am.* **58**, 539-545 (1968).

[23]C. L. Rino, "Bandlimited Image Restoration by Linear Mean-Square Estimation," *J. Opt. Soc. Am.* **59**, 547-553 (1969).

[24]T. M. Cannon, H. J. Trussell, and B. R. Hunt, "Comparison of Image Restoration Methods," *Appl. Opt.* **17**, 3384-3390 (1978).

[25]T. G. Stockham, Jr., "Image Processing in the Context of a Visual Model," *Proc. IEEE* **60**, 828-842 (1972).

[26]W. K. Pratt, "Generalized Wiener Filtering Computation Techniques," *IEEE Trans. Comp.* **C-21**, 636-641 (1972).

[27]D. B. Harris, J. H. McClellan, D. S. K. Chan, and H. W. Schuessler, "Vector Radix Fast Fourier Transform," IEEE Conf. on Acoustics, Speech, and Signal Processing, Hartford, Conn. (May 9-11, 1977).

[28]B. R. Frieden, "Unified Theory for Estimating Frequency-of-Occurrence Laws and Optical Objects," *J. Opt. Soc. Am.* **73**, 927-938, (1983).

[29]E. S. Meinel, "Origins of Linear and Nonlinear Recursive Restoration Algorithms," *J. Opt. Soc. Am.* **3**, 787-799 (1986).

# INITIAL DISTRIBUTION EXTERNAL TO THE APPLIED PHYSICS LABORATORY*

The work reported in TG 1368 was done under Navy Contract N00039-87-C-5301 and is related to Task M2Q0, supported by the Naval Air Systems Command.

| ORGANIZATION | LOCATION | ATTENTION | No. of Copies |
|---|---|---|---|
| DEPARTMENT OF DEFENSE | | | |
| Office of the Secretary of Defense | Washington, DC 20301 | OUSDRE(ET) | 1 |
| Defense Technical Information Center | Alexandria, VA 22314 | Accessions | 12 |
| DEPARTMENT OF THE NAVY | | | |
| Office of Chief of Naval Operations | Washington, DC 20350 | | |
| Director, Res., Dev., and Acq. | | OP-98 | 1 |
| Director, Technology Assessment Div. | | OP-987 | 1 |
| Deputy Chief Scientist | | OP-987B | 1 |
| Director, Surface Combat Systems Div. | | OP-35 | 1 |
| Electro-Optics Adv. | | OP-35E | 1 |
| Dep. Chief, Naval Operations | | OP-507D | 1 |
| Office of Asst. Secretary of the Navy (RE&S) | Washington, DC 20350 | R. L. Rumpf | 1 |
| NAVAIRSYSCOM | Washington, DC 22202 | | |
| Planning and Programming Br. | | AIR-9301 | 1 |
| Tech Transfer Manager | | AIR-9303A | 1 |
| Director, Weapons Div. | | AIR-932 | 1 |
| ASM, Weapons Div. | | AIR-932A | 1 |
| Weapons Guidance | | AIR-932G | 1 |
| APM HARPOON | | AIR-5402D | 1 |
| Prog. Mgr. Anti-Ship Weapon Sys. | | PMA-258 | 1 |
| | | PMA-280 | 1 |
| | | PMA-280A | 1 |
| Library | | AIR-7226 | 2 |
| NAVSEASYSCOM | Washington, DC 22202 | | |
| Research Technology and Assessment Ofc. | | CET-1 | 1 |
| Director, Weapons & Combat Systems | | SEA-06 | 1 |
| Executive Director | | SEA-06B | 1 |
| Surface Warfare Systems Group | | SEA-62B | 1 |
| Surface Missile Systems Subgroup | | SEA-62Z | 1 |
| Long Range Missile Systems Div. | | SEA-62Z1 | 1 |
| Medium Range Missile Systems Div. | | SEA-62Z2 | 1 |
| Guided Missile Div. | | SEA-62Z3 | 1 |
| Technical Director | | SEA-62Z3B | 1 |
| Library | | SEA-9961 | 2 |
| NAVPRO | Laurel, MD 20707 | | 1 |
| COMMANDS & CENTERS | | | |
| Naval Supply Systems Command | Washington, DC | NSUP-03412A | 1 |
| Naval Ocean Systems Command | San Diego, CA | 0141 | 1 |
| SPAWAR | Washington, DC | SPAWAR-32T | 1 |
| Naval Avionics Center | Indianapolis, IN | 803 | 1 |
| David W. Taylor Naval Ship R&D Center | Bethesda, MD | 012.2 | 1 |
| Naval Air Development Center | Warminster, PA | 7012 | 1 |
| Naval Weapons Center | China Lake, CA | 3942 | 1 |
| Naval Surface Weapons Center | White Oak, MD | D21 | 1 |
| Office of Naval Technology | Arlington, VA | OCNR-26 | 1 |
| Naval Research Laboratory | Washington, DC | 1001 | 1 |
| | | 6500 | 1 |
| | | 6530 | 1 |
| | | 6570 | 1 |
| Naval Post Graduate School | Monterey, CA | 62TV | 1 |
| DEPARTMENT OF THE ARMY | | | |
| U.S.A. Night Vision and Electro-Optics Lab. | Fort Belvoir, VA | DELNV-RM-RA | 1 |
| GOVERNMENT AGENCIES | | | |
| National Security Agency | Ft. George G. Meade, MD | R022 | 1 |
| Miscellaneous | | | |
| SAIC | 5151 E. Broadway<br>Tucson, AZ 85711-3796 | B. R. Hunt | 1 |

**Requests for copies of this report from DoD activities and contractors should be directed to DTIC, Cameron Station, Alexandria, Virginia 22314 using DTIC Form 1 and, if necessary, DTIC Form 55.**

*Initial distribution of this document within the Applied Physics Laboratory has been made in accordance with a list on file in the APL Technical Publications Group.